Mutational and Crystallographic Analyses of Interfacial Residues in Annexin V Suggest Direct Interactions with Phospholipid Membrane Components[†,‡]

B. Campos,[§] Y. D. Mo,[||] T. R. Mealy,[||] C. W. Li,[||,⊥] M. A. Swairjo,[||,#] C. Balch,[§,▽] J. F. Head,[||] G. Retzinger,[○] J. R. Dedman,[§] and B. A. Seaton*[,||]

Departments of Molecular and Cellular Physiology and of Pathology and Laboratory Medicine, University of Cincinnati, College of Medicine, 231 Bethesda Avenue, Cincinnati, Ohio 45220, and Structural Biology Group, Department of Physiology, Boston University School of Medicine, 80 East Concord Street, Boston, Massachusetts 02118

Received December 23, 1997; Revised Manuscript Received April 1, 1998

ABSTRACT: Annexin V belongs to a family of eukaryotic calcium-dependent membrane-binding proteins. The calcium-binding sites at the annexin−membrane interface have been investigated in some detail; however, little is known about the functional roles of highly conserved interfacial residues that do not coordinate calcium themselves. In the present study, the importance of tryptophan 185, and threonine or serine at positions 72, 144, 228, and 303, in rat annexin V is investigated by site-directed mutagenesis, X-ray crystallography, and functional assays. The high-resolution crystal structures of the mutants show that the mutations do not cause structural perturbations of the annexin molecule itself or disappearance of bound calcium ions from calcium-binding sites. The assays indicate that relative to wild-type annexin V, loss of the methyl substituent at position 72 (Thr72→Ser) has no effect while loss of the hydroxyl group (Thr72→Ala or Thr72→Lys) causes reduction of membrane binding. Multiple lysine substitutions (e.g., Thr72,Ser144,Ser228,Ser303→Lys) have a greater adverse effect than the single lysine mutation, suggesting that in annexin V the introduction of potentially favorable electrostatic interactions between the lysine side chains and the net negatively charged membrane surface is not sufficient to overcome the loss of the hydroxyl side chains. Replacement of the unique tryptophan, Trp185, by alanine similarly decreases membrane binding affinity. Taken together, the data suggest that the side chains mutated in this study contribute to phospholipid binding and participate directly in intermolecular contacts with phospholipid membrane components.

The annexins are a family of eukaryotic calcium-dependent membrane-binding proteins. The proposed in vivo functions of the annexins relate to their membrane-binding properties and include roles in exocytosis and membrane trafficking, ion channel activity, cell growth and proliferation, cell adhesion, inflammation, and related processes (for review, see *1*−*4*). Annexin sequences show strong homology, containing four (or eight, in annexin VI) canonical domains in a conserved core that confers calcium-dependent membrane-binding properties common to the family. Annexin V, a 35 kDa monomeric protein, has been studied widely in terms of tertiary structure and membrane-binding properties and provides an excellent opportunity for investigation of protein−lipid interfacial interactions.

Several aspects of annexin V binding to membranes have been reported. The orientation of annexin V with respect to the membrane has been well characterized, as have some details of the binding interactions. High-resolution electron microscopy of two-dimensional annexin crystals on phospholipid monolayers indicates that annexin V lies flat along the membrane surface, with relatively little insertion into the bilayer (*5*, *6*). Membrane-bound annexin V self-associates, forming trimers and higher aggregates along the membrane surface (*7*, *8*). The high-affinity membrane−annexin V association (K_d < nM; *9*) requires calcium and a negatively charged membrane component, typically an anionic phospholipid such as phosphatidylserine (PS).[1] As with other annexins, hierarchical preferences among phospholipids are observed (*10*), though the structural basis for selective binding is not clear. On a molecular level, crystallographic

[†] Supported by NIH Grants GM-55445 (B.A.S.) and DK-46433 (J.R.D.).

[‡] Coordinates will be deposited in the Protein Data Bank (codes: 1bc0, 1bcw, 1bcy, 1bcz, 1bc1, 1bc3).

* To whom correspondence should be addressed.

[§] Department of Molecular and Cellular Physiology, University of Cincinnati.

[||] Boston University School of Medicine.

[⊥] Present address: Amgen, Thousand Oaks, CA 91320.

[#] Present address: Smith-Kline Beecham Pharmaceuticals, King of Prussia, PA 19406.

[▽] Present address: Trevigen Inc., Gaithersburg, MD 20877.

[○] Department of Pathology and Laboratory Medicine, University of Cincinnati.

[1] Abbreviations: PS, phosphatidylserine; EGTA, ethylene glycol bis-(β-aminoethyl ether)-*N*,*N*,*N*′,*N*′-tetraacetic acid; HEPES, *N*-(2-hydroxyethyl)piperazine-*N*′-2-ethanesulfonic acid; PC, phosphatidylcholine; PE, phosphatidylethanolamine; aPTT, activated partial thromboplastin time; PBS, phosphate-buffered saline; DTT, dithiothreitol; SUVs, small unilamellar vesicles; LUVs, large unilamellar vesicles; W185A, Trp185→Ala site-directed mutant; T72A, Thr72→Ala site-directed mutant; T72S, Thr72→Ser site-directed mutant; T72K, Thr72→Lys site-directed mutant; T72,S144,S228-(K), Thr72,Ser144,Ser228→Lys triple site-directed mutant; T72,S144,S228,S303-(K), Thr72,Ser144,Ser228,-Ser303→Lys quadruple site-directed mutant.

S0006-2960(97)03142-5 CCC: $15.00
Published on Web 05/12/1998

Table 1: Annexin Sequence Homology at Positions Equivalent to 72, 144, 228, and 303 in Rat Annexin V [Sequence Data from (*12*) and (*47*)]

domain				
I (72)	II(144)	III(228)	IV(303)	annexin: source
T	S	S	S	V: rat, human, chicken, bovine VIa: human, mouse
S	S	S	S	III: human, rat IV: human, bovine VIb: human, mouse VII: human XI: human XIII: human, dog XII: hydra* XIV: *Dictyostelium*[a] XVI: *C. elegans*[a]
S	S	S	K	XV: *C. elegans*[a]
T	S	K	K	I: human, mouse, rat, guinea pig, sponge
S	S	K	K	II: human, bovine, mouse I: pig
K	S	K	K	I: pigeon

[a] No mammalian annexin counterpart.

data indicate that the membrane facing surfaces of annexins contain numerous calcium-binding sites (*11*−*13*) and that "calcium bridges" form between protein and phospholipid headgroup (*14*, *15*). The importance of calcium binding to the annexin−membrane association has been probed in previous site-directed mutagenesis experiments (*16*−*22*). None of these studies included crystallographic analysis.

Since so much of the putative membrane-binding surface of annexin V consists of calcium-binding loops, the identity of other surface residues that interact directly with membrane components has been difficult to distinguish in mutagenesis experiments. Mutations that even indirectly alter calcium binding may also affect membrane-binding properties, without any direct contact between the mutated residue and phospholipid membrane. Moreover, some mutations may exert the greatest effect at a distant rather than local site, since important interactions exist between calcium-binding loops. As the mutation of surface residues is unlikely to result in significant changes in conformation, disruption of calcium sites is unlikely to be detected using methods such as circular dichroism. To avoid this uncertainty, the present studies use X-ray crystallography to accurately assess the structural consequences of the site-directed mutagenesis experiments on interfacial residues in annexin V.

Targets for mutagenesis in this study were suggested by patterns of sequence conservation among annexins (Table 1) and available crystallographic data. In particular, several highly conserved residues that occur on the membrane-binding surface but do not appear to participate in calcium coordination were postulated to serve as membrane-binding determinants. The interfacial surface of annexin V is principally hydrophilic, though certain surface-exposed hydrophobic residues may play a role in membrane binding. One of these residues, tryptophan 185[2] in the third domain, exhibits a large-scale calcium-dependent conformational change in which the side chain moves from a buried position in the protein interior to protrude outward from the protein surface (*13*, *23*). Fluorescence data indicate that the Trp185 side chain interacts directly with the phospholipid membrane (*24*, *25*). In the present work, Trp185 has been mutated to alanine (W185A) to test the effects of this substitution on annexin−membrane binding.

In addition to Trp185, the other mutations reported herein probe the function of a highly conserved hydroxyl group found in equivalent positions in each domain: threonine 72, serine 144, serine 228, and serine 303 (Table 1). In annexin V crystal structures, the side chains of these four residues form no important contacts with amino acids, ions, or solvent molecules. This observation suggests that these hydroxyl-amino acids make important interactions with phospholipid molecules since there is no evidence to indicate a structural role. In the present study, these residues are mutated to alanine, serine (for Thr72), or lysine to test the importance of the hydroxyl group at this position. The alanine and serine mutations were made to probe the relative contributions of the hydroxyl and methyl groups, respectively, of Thr72. The lysine mutation was made to change the charge at this position from neutral to positive. In annexins I and II, lysine naturally occurs at positions where hydroxyl-amino acids are found in annexin V (Table 1), suggesting a priori that this substitution would be structurally benign and that subtle membrane-binding effects might be caused by the mutation.

MATERIALS AND METHODS

Mutagenesis Procedure. The 1.5 kb fragment of the annexin V cDNA obtained from B. Pepinsky, Biogen, was cloned in the *Nco*I site of the Pharmacia Biotech expression vector pKK233-2, which contains the hybrid trc promotor and the gene for ampicillin resistance. Site-directed mutagenesis was then performed using the Clontech transformer site-directed mutagenesis kit. To produce the T72 mutants, the ACC (coding for threonine) codon was changed to AAG (lysine), GCC (alanine), or CCT (serine). For W185A, the TGG (tryptophan) codon was changed to GCC. The triple mutant T72,S144,S228-(K) substituted lysine (codon TTT) for T72, S144 (codon TCT) and S228 (codon TCA). The quadruple mutant T72,S144,S228,S303-(K) substituted lysine (codon AAG) for T72S, S144, S228, and S303 (codon TCT). The presence of the desired mutation in the final plasmid construct was verified by double-strand DNA sequence analysis.

[2] Numbering is that of rat annexin V unless otherwise indicated; Trp185 corresponds to Trp187 in human annexin V.

Protein Expression and Purification. Cultures of *Escherichia coli* strain JM101 containing rat annexin V cloned in the Pharmacia expression vector pKK233-2 were grown overnight at 37 °C in Bio 101 LB medium with 100 μg/mL ampicillin and then diluted 100-fold into fresh LB medium with 100 μg/mL ampicillin. When the optical density at 600 nm reached a value of 0.3−0.5, isopropyl β-D-thiogalactopyranoside is added to a final concentration of 1 mM and growth continued for 4 h. Bacteria are harvested by centrifugation, and pellets are stored at −20 °C overnight. For purification, frozen pellets are thawed and suspended in lysis buffer (50 mM Tris-HCl, pH 8.0, 1 mM EDTA, 100 mM NaCl). Samples are sonicated on ice and subjected to three freeze/thaw cycles. Samples from the last thaw are transferred to centrifuge tubes, spun for 30 min at 12000*g* and then for 1 h at 150000*g* and concentrated by spinning for 1 h at 5000*g* through an Ultrafree-15 centrifugal filter device (Millipore). Thirty-five milliliters of concentrate is dialyzed against EGTA buffer (0.1 M NaCl, 50 mM HEPES, pH 7.4, 2.5 mM EGTA). After column equilibration with $CaCl_2$ buffer (0.1 M NaCl, 50 mM HEPES, pH 7.4, 1 mM $CaCl_2$), the dialysate is passed over a lipid affinity column, prepared as described previously (*26*), of small unilamellar vesicles composed of PS/PC/PE (2:2:1) coupled to cyanogen bromide-activated Sepharose 4B. The protein-bound column is washed again with 300 mL of $CaCl_2$ buffer, and then switched to EGTA buffer. Approximately 50 mL of eluate is collected dropwise at a flow rate of 0.5 mL/min. The eluate is concentrated to 2−4 mL in volume in an Amicon Centricon-10 centrifugal filter device, dialyzed against 3 L of 1/50 buffer (0.1 M KCl, 50 mM HEPES, pH 7.4, 0.02% NaN_3, 0.1 mM DTT), and washed by three cycles of spinning/diluting in annexin buffer to a final volume of 1−2 mL to be used for assays. Protein concentration was measured by using the Pierce BCA protein assay.

Fluorescence Phospholipid-Binding Assay. Binding of wild-type and mutant annexin V proteins was determined by a fluorescent phospholipid self-quenching assay (*27*). To perform this assay, large unilamellar vesicles (100 nm) containing 85 mol % Sigma Chemical brain phosphatidylcholine and 15 mol % 1-18:1,2-C_{12}-NBD-PS were prepared by drying phospholipid under nitrogen and resuspending in HEPES-buffered saline (HBS: 10 mM HEPES, 0.9% NaCl, pH 7.4) at a concentration of 1 mM total lipid. This solution was then passed 10 times through a Lipex extruder using Costar 100-nm pore-size filters, according to the method of Hope et al. (*28*).

The fluorescence assay is based upon self-quenching of the NBD chromophore induced by annexin V-induced clustering of phospholipids (*27*). In this assay, the greater the percent quenching of NBD-PS, the greater the membrane binding affinity. In this method, 10 μM fluorescent liposomes in HBS and 1 mM $CaCl_2$ were placed in a cuvette (2 mL total volume) and measured at an excitation wavelength of 465 nm and emission wavelength of 530 nm using a Perkin-Elmer LS-5B spectrofluorometer. The change in fluorescence intensity was then measured as a function of protein concentration. The percent quenching was calculated by the equation: $[(F_o - F)/F_o] \times 100$, where F_o is the initial fluorescence intensity prior to protein addition and F is the fluorescence intensity following addition. To assess the calcium dependence of quenching, the solution was adjusted to 3 mM EGTA following protein titration. All fluorescence measurements were corrected for dilution.

Centrifugation Assay (Ca^{2+} Concentration at Half-Maximal Membrane Binding). Small unilamellar vesicles (SUVs) of 1:1 mixtures of DOPS/DOPC (Avanti Polar Lipids) were prepared by drying lipid/chloroform solutions under nitrogen, followed by rotary evaporation and suspension in buffer (0.1 M KCl, 50 mM HEPES, pH 7.4, 0.02% NaN_3, 0.1 mM DTT) to a final concentration of 5−10 mM. The lipid suspensions were extruded through an Avestin 100 nM membrane pore size LiposoFast homogenizer 15−19 times. The final phospholipid concentrations were determined by a phosphate ashing procedure (*29*). A centrifugation assay described previously (*94*) was used to estimate the avidity of calcium-dependent phospholipid binding by the protein. Briefly, mixtures of annexin V and phospholipids in a range of $CaCl_2$ concentrations in 5−10 μM increments were incubated for 15 min and then centrifuged through a Centricon-100 filtering device at 1000*g* for 45 min. The first filtrate was reserved for analysis by SDS−PAGE. The retentates, which contain the bound protein fraction, were washed once, resuspended in buffer, and subjected to SDS gel electrophoresis. This assay provides the calcium concentration at which the relative band intensities of filtrate and retentate are approximately equal, as detected by eye and by densitometry. The lower this calcium concentration, the better the adsorption of annexin to membrane is presumed to be. These measurements are imprecise but reliable in providing qualitative, if not quantitative, data. To establish binding hierarchies in the present studies, assays in triplicate on different mutants were performed in parallel and compared with wild-type, using the same vesicles and buffer solutions.

Blood Coagulation Assay. Prolongation of clotting time (activated partial thromboplastin time, aPTT) induced by annexin V, a potent in vitro inhibitor of blood coagulation, was measured for wild-type and mutant proteins. Activated partial thromboplastin times (aPTT) were obtained using citrated (13 mM), normal pooled plasma, Dade actin FSL according to a modification of Fritsma (*31*). Briefly, 50 μL of PBS (0.15 M Na^+, 10 mM PO_4^{2+}, pH 7.4) containing a precise quantity of annexin was mixed with an equivalent volume of aPTT reagents. The mixture was incubated at 37 °C for 30 min, after which 50% of the mixture was then used to determine the aPTT of normal pooled plasma. Shorter aPTT values are consistent with weaker membrane binding by annexin V.

Crystallization, Structure Determination, and Refinement. The rat annexin V wild-type or mutant proteins were crystallized at 17 °C by vapor diffusion against a reservoir of 34−40% saturated ammonium sulfate, 50 mM HEPPS buffer, pH 8.2, 0.02% NaN_3, 2 mM dithiothreitol, and 10 mM $CaCl_2$. The final protein and calcium concentrations at equilibration were 14 mg/mL and 20 mM, respectively. Crystals belonged to the *R3* space group with a monomer in the asymmetric unit, as described previously (*32*). Data were collected in 1.5° oscillation frames on an R-Axis IIc imaging plate detector with a Molecular Structure Corp. cryo system mounted on a Rigaku RU-300 rotating anode generator. Data were collected from a single crystal and processed using DENZO and SCALEPACK (*33*). Mutant data sets initially were refined in X-plor (*34*) using a high-resolution crystal

Table 2: Crystallographic Data Collection and Refinement Statistics

data set	W185A	T72S	T72A	T72K	triple[a]	quad[a]
data collection						
unit cell dimensions (R3)						
$a = b$ (Å)	157.30	157.37	157.67	157.39	157.34	157.32
c (Å)	37.01	36.82	36.92	37.42	37.59	37.49
no. of unique reflections	19780	14209	16916	21238	21029	17154
redundancies	2.6	3.5	3.4	4.8	3.0	3.0
applied resolution limit (Å)	2.00	2.20	2.10	1.95	1.95	2.05
completeness (%)	86.2	83.2	85.6	84.9	83.7	79.8
R_{merge}[b]	13.3	11.3	13.4	9.8	11.0	11.2
refinement:						
R_{xray}[c]	0.226	0.227	0.227	0.222	0.211	0.209
R_{free}[c]	0.296	0.299	0.256	0.292	0.259	0.254
mean *B*-factors (Å^2), main chain/side chain	22.7/26.3	28.6/31.8	28.7/31.8	23.6/27.3	23.5/28.0	16.9/19.8
no. Ca^{2+}/SO_4^{2-} ions/water molecules	5/1/131	5/1/106	5/1/130	5/1/129	5/1/109	5/1/115
*r*msd,[e] bond						
lengths (Å)	0.020	0.008	0.018	0.007	0.005	0.014
angles (deg)	1.909	1.243	1.758	1.060	1.183	1.671
rmsd, angles (deg)	22.585	22.929	22.555	22.183	22.019	22.237
dihedral/improper	1.101	0.614	0.937	0.548	0.576	0.828
rmsd from WT[f]						
all atoms	0.756	0.757	0.753	0.758	0.748	0.753
Cα only (Å)	0.283	0.296	0.272	0.274	0.318	0.396

[a] Triple = T72,S144,S228-(K). Quadruple = T72,S144,S228,S303-(K). [b] $R_{merge} = \sum|I_i - \langle I\rangle|/\sum I_i \times 100$ where I_i is the intensity of an individual reflection and $\langle I\rangle$ is the mean intensity of that reflection. [c] $R_{cryst} = \sum||\boldsymbol{F}_P| - |\boldsymbol{F}_{calc}||/\sum|\boldsymbol{F}_P| \times 100$ where $|\boldsymbol{F}_{calc}|$ is the calculated structure factor.[d] R_{free} is as defined in Brünger (*35*). [e] rmsd = root-mean-square deviation. [f] Wild-type rat annexin V (*13*).

structure of wild-type annexin V from crystals grown under similar conditions. Refinement using rigid-body, positional, and simulated annealing protocols was monitored by R_{free} (*35*) and R_{cryst} values, and manual intervention using the graphics program O (*36*) was employed as needed. The X-plor refined model was introduced into CCP4 (*37*) for further refinement and automatic water fitting. Density is lacking for the N-terminal formylmethionine, which is omitted from all models. At various stages, the model geometry was checked using Procheck (*38*) to guide the refinement and rebuilding. Iterative cycles of X-plor/CCP4 refinement brought the final statistics to those shown in Table 2.

RESULTS

Binding of Annexin V Mutants to LUVs Containing Synthetic PS/PC. The same relative affinities for LUVs, i.e., membrane binding hierarchies, were obtained for the annexin V mutants using either fluorescence quenching or centrifugation assays. The fluorescence quenching data are given in Figure 1. The multiple site mutants, i.e., triple mutant T72,S144,S228-(K) and quadruple mutant T72,S144,S228,-S303-(K), bound to vesicles more weakly than any single point mutant. Substitution at position 185 weakened binding more than those at position 72. Of the three T72 substitutions, the lysine substitution (T72K) produced a significant reduction in binding affinity. Wild-type, T72S, and T72A had similar maximal binding capacities. The centrifugation assay ordered the membrane binding of the mutants as wild-type ≈ T72S > T72A > T72K > W185A > T72,S144,S228-(K) ≈ T72,S144,S228,S303-(K).

Anticoagulation Assay. While not a direct measure of membrane binding affinity, anticoagulation by annexin V is closely correlated with its ability to bind acidic membranes (*39*). Figure 2 shows the aPTT data for annexin V wild-type and mutant proteins. The multiple mutants showed no significant anticoagulation activity. The T72K and W185A

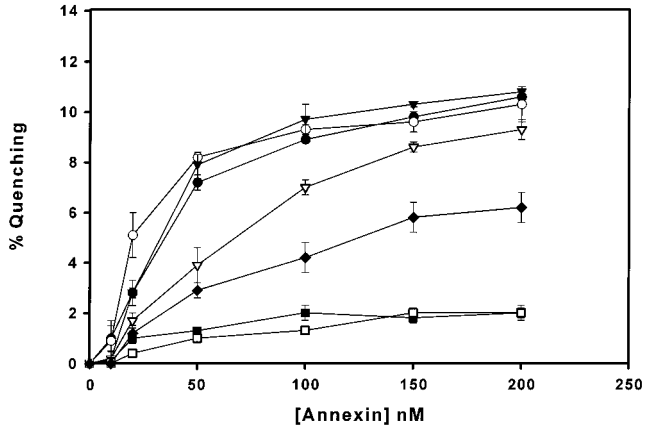

FIGURE 1: Fluorescence assay of membrane binding by annexin V wild-type and mutants. Measurements were obtained using a 95% confidence level ($p = 0.05$). Symbol key: solid circles, wild-type; open circles, T72A; solid triangles, T72S; open triangles, T72K; solid squares, T72,S144,S228-(K); open squares, T72,S144,S228, S303-(K); diamonds, W185A.

mutants yielded a slight reduction in clotting time, but clots still formed at the highest annexin concentrations tested. Wild-type, T72S, and T72A completely prevented clotting at the higher annexin concentrations assayed. The T72S mutant proved to be a very strong anticoagulant: of the proteins tested, T72S completely prevented clotting at the lowest annexin concentration. The reason for this high anticoagulation is unclear because unlike the other two assays aPTT measurements involve a complex mixture of proteins in plasma, not just annexin and liposomes.

Crystallographic Analysis. Crystal structures were obtained for each of the annexin V mutants to assess whether the mutations induce global or local structural perturbations. The small rms deviations of these structures from wild-type (Table 2) and each other are consistent with no conformational differences between wild-type and mutant proteins. The mutated residues occur on the protein surface where they

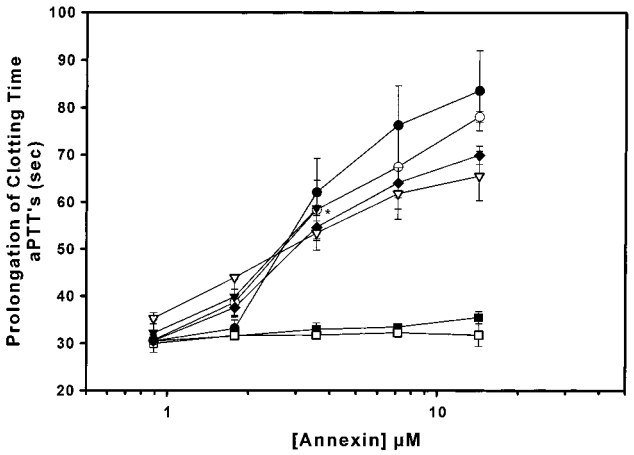

FIGURE 2: Blood coagulation (aPTT) assay of annexin V wild-type and mutants. Symbol key: solid circles, wild-type; open circles, T72A; solid triangles, T72S; open triangles, T72K; solid squares, T72,S144,S228-(K); open squares, T72,S144,S228,S303-(K); diamonds, W185A. For T72S, no clotting was detected beyond the point marked with an asterisk.

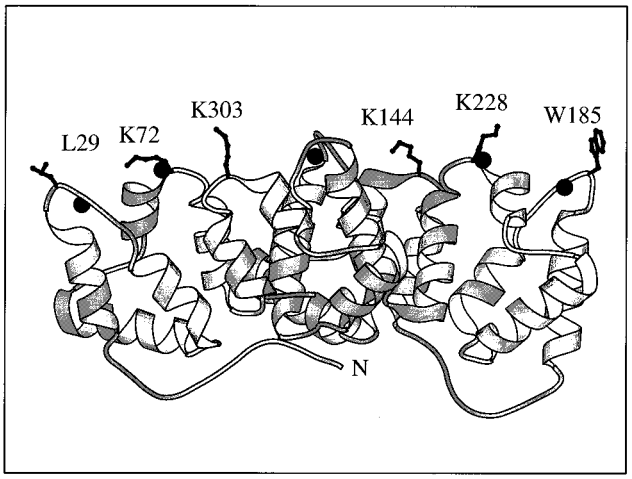

FIGURE 3: Ribbon diagram of the crystal structure of the quadruple mutant, T72,S144,S228,S303-(K), showing mutated lysine side chains and hydrophobic side chains of Leu29 and Trp185. In this orientation, the membrane adsorption surface of annexin V faces up. Calcium ions are shown as solid spheres. Figure prepared with MOLSCRIPT (*48*).

interact principally with solvent and/or side chains of molecules related by crystallographic symmetry (Figure 3). Of the four Ser/Thr→Lys substitutions, Lys72 and Lys144 side chains each fold back toward the protein surface to hydrogen-bond with the main-chain oxygen of residues 70 and 142, respectively. The side chains of Lys228 and Lys303 each extend away from the protein surface and across a solvent channel to form salt-bridges with Asp167 or Asp318, respectively, of a symmetry-related molecule. Ala185 also extends out toward solvent and occupies the same relatively hydrophobic environment, formed by side chains (e.g., Leu183) of symmetry-mates, as did Trp185 in the wild-type protein. None of these new contacts appears to influence local structure nor are any important contacts lost through mutation of the wild-type residues.

The calcium-binding sites, particularly those near the mutated residues, were given particularly close scrutiny in terms of altered structure. Superposition of Cα calcium-binding loops alone, whether mutated or not, gave smaller rms deviations than for all Cα atoms. The number of calcium atoms and the intensity of their peaks (derived from sigma levels in $F_o - F_c$ maps) did not vary significantly in any structure. Calcium ions were identified from $F_o - F_c$ maps (where F_c refers to protein alone). Criteria used to differentiate calcium from solvent were peak intensity (typically $4-5\sigma$ or more, where σ is that of the difference map) and *b*-factors, geometry (appropriate ligands and bond lengths), and observation in previous rat annexin V wild-type crystal structures (*13*, *15*). By these criteria, each mutant structure contained five calcium ions and one sulfate ion. The metal ions were bound at the 1AB[3] (residues 26−30, 70) and 1DE (68−76) domain I calcium-binding sites (Figure 4), the 3AB (181−186, 226) and 3DE (224−232) domain III sites, and the 4AB (257−261, 301) domain IV sites. Peak intensity was observed at positions corresponding to other previously identified calcium sites; however, these did not possess the requisite intensity or geometry for calcium ions and may represent sites with low calcium occupancy in these crystals. The sulfate ion was located in domain I, near the binding site of the AB loop calcium ion.

DISCUSSION

Most of the mutations evaluated in this study led to a reduction of membrane binding. Three different assays were used to assess membrane binding affinity, as formation of the annexin−Ca^{2+}−membrane ternary complex is difficult to measure directly. The fluorescence and aPTT assays measure annexin properties for which membrane binding is requisite, i.e., clustering of membrane phospholipids and inhibition of blood coagulation. The centrifugation assay measures the apparent calcium dependence of ternary complex formation in synthetic vesicles, a macroscopic property. The assay cannot give a direct measure of the calcium binding affinity of the protein in the ternary complex as it includes the contribution of an unknown number of heterogeneous calcium-binding sites. However, the presence of bound calcium ions is indicated by their observed electron density in the crystal structures. The combined data thus provide a comparative measure of the relative strength of membrane binding of annexin V wild-type and mutant proteins. In all assays, the W185A and T72K mutants exhibited the weakest membrane binding of the single-site mutants. The T72S mutant performed as well as or, in the case of anticoagulation, better than wild-type annexin V. In the centrifugation assay, the T72A mutant clearly bound less well at lower calcium levels than either the T72S or the wild-type proteins and did not express the same degree of anticoagulation as the T72S mutant. In all three assays, multiple lysine substitutions caused the greatest reduction in membrane binding affinity.

The crystallographic data indicate that the protein conformations of the mutants are virtually indistinguishable from that of wild-type annexin V. In particular, no significant differences can be seen in the calcium-binding loops. These structural data are important because if any mutation eliminated one or more bound calcium ions, fewer calcium bridges could be expected to form and membrane binding

[3] Nomenclature: AB and DE loops, which contain calcium-binding sites, separate the antiparallel A and B helices, and the D and E helices, respectively; Roman numerals refer to domains.

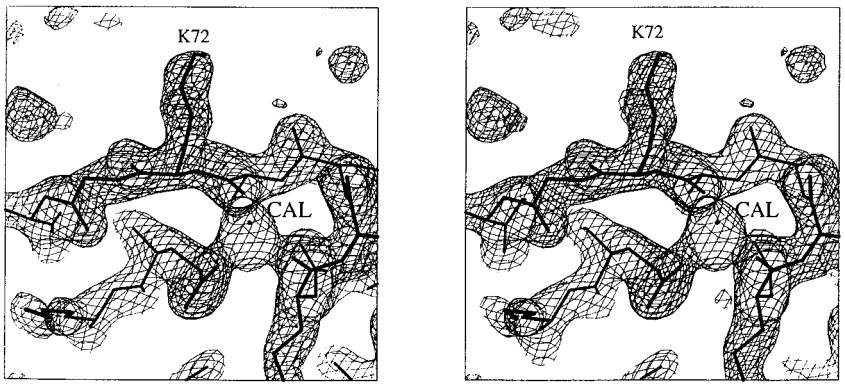

FIGURE 4: Stereoview of $2F_o - F_c$ electron density map at 1σ of T72K mutant. The orientation is similar to that in Figure 3, with slight (5−10°) rotation around the *x* and *y* axes for clarity. Shown is the domain I DE loop with the lysine mutation at position 72 and the 1DE calcium ion. Map calculated in X-plor (*34*), figure prepared in O (*36*).

would be weakened commensurately. In this case, the effect of the mutation would be secondary to the loss of calcium binding, and little information would be obtained about the functional role of the mutated residue itself in membrane binding. The crystallographic data in the present studies indicate that the mutant proteins have the same structure and calcium ions bound as the wild-type protein. Therefore, the consequences of any mutation in terms of changed behavior in assays directly reflect the implied role of the substituted side chain in annexin−membrane binding. The implications of these structure−function correlations will be discussed in turn.

Tryptophan side chains in membrane proteins have been shown to distribute asymmetrically to the protein−membrane interface, where many perform functional roles (*40*). In annexin V, the loss of the unique tryptophan in the W185A mutant is associated with reduced membrane affinity in all three assays. The simplest explanation for the biochemical behavior of the W185A mutant is that favorable interactions are lost between the tryptophan aromatic ring and membrane components. Fluorescence studies have provided evidence that the Trp185 side chain resides at the interfacial region, where specific contacts are made with the phospholipid polar head region (*14*, *24*, *41*). The crystal structure of annexin V complexed with phospholipid headgroup analogues reveals close contacts between the glycerol backbone and the Trp185 side chain (*15*), in good agreement with the fluorescence results. Recent time-resolved fluorescence studies show that the interfacially located tryptophan side chain may be in equilibrium with another conformation that penetrates into the lipid bilayer (*25*). Another possible function of the Trp185 side chain may be to position the annexin molecule along the membrane surface to maximize favorable interfacial contacts. Bilayer insertion of the hydrophobic side chains of Trp185 and its positional equivalent, Leu29 (Figure 3), thus could effectively anchor the protein to the membrane surface in the proper orientation (*8*).

The present data on the conserved serine/threonine residues provide further information on the role of the calcium-binding DE loops, which have not been investigated extensively to date. The DE loops form shallow grooves along the membrane-facing surface of the protein and bind calcium more weakly than the AB loops, where Leu29 and Trp185 are located. Only acidic calcium-binding DE loop residues have been mutated previously, with loss of associated properties (*18*, *22*). In the present work, mutation of positionally equivalent DE loop residues Thr72, Ser144, Ser228, and Ser303 reduces membrane absorption but not by disrupting local Ca^{2+} binding. These results suggest that in the wild-type protein, the side chain hydroxyl groups at these positions make contact and interact favorably with membrane phospholipids.

The role(s) of basic residues in interfacial binding in annexins is (are) also addressed in the present studies. Several peripheral membrane-associated proteins, including phospholipase A_2 (*42*), myristolated proteins such as MARCKS (*43*), and β_2-glycoprotein (apolipoprotein H; *44*), have polybasic clusters that participate in interfacial binding to anionic membranes. For annexins, other structural features have been identified in the present work and elsewhere as playing central roles in protein−membrane association. Predictive models of binding between extrinsic proteins and anionic membranes suggest that at least two distinct processes contribute to macroscopic binding affinity: nonspecific adsorption of protein to the membrane surface, followed by specific interactions between acidic lipids and protein residues (*45*, *46*). For annexins, there is considerable evidence to suggest that protein adsorption to anionic membranes is driven by electrostatics. However, annexins also recognize certain structural features of membrane phospholipids, and these interactions contribute substantively to macroscopic membrane binding affinity. Meers and Mealy (*14*) point out that after saturating nonspecific components of binding with an excess of negative charge, the binding of micelles to annexins is strongly dependent on specific interactions with certain phospholipid moieties, e.g., the SN-2 acyl chain.

The adverse effect on macroscopic annexin V−membrane binding of lysine substitutions for neutral, polar amino acids suggests that of the two processes contributing to macroscopic binding, specific interactions between protein and membrane can, in some cases, outweigh electrostatic contributions to nonspecific adsorption. Further, the balance between the two processes may vary among annexins since their interfacial surfaces and membrane-binding properties differ. For example, native annexins I and II contain lysine at some of the positions equivalent to the conserved serine/threonine residues in annexin V (Table 1). As compared with annexin V, annexins I and II are better at binding the acidic phospholipids, phosphatidic acid and phosphati-

dylserine, but worse at binding phosphatidylethanolamine (*10*). These observations are consistent with site-directed mutagenesis data showing that substitution of a lysine (not listed in Table 1) for glutamate in annexin I reduces overall membrane binding but enhances phosphatidylethanolamine binding affinity (*20*). These data suggest that in annexins I and II, surface lysines play an important electrostatic role by enhancing binding to acidic phospholipids and perhaps repelling the positively charged ethanolamine moiety of PE. Electrostatics alone would predict that annexin V mutated to include additional lysine side chains should exhibit binding preferences similar to annexins I and II; yet this is not observed.

At least in the case of annexin V, specificity may be more important than nonspecific electrostatics in determining macroscopic membrane binding affinity. Comparative binding studies show that while annexins I and II bind acidic phospholipids better than does annexin V, discrimination between these lipids is considerably greater in the latter. The range in free Ca^{2+} concentrations for half-maximal binding of acidic phospholipids by annexins I and II is fairly narrow: 0.6, 1.3, 2.0 μM (annexin I) and 0.2, 0.65, 1.3 (annexin II), for PA, PS, or PI, respectively. In contrast, the range for annexin V is much wider: 1.2, 16, 130 μM. Further comparison with annexins III, IV, and VI shows that annexin V shows the greatest degree of discrimination, i.e., the widest range (>100-fold), among these acidic phospholipids (*10*). This preferential binding cannot be explained simply by the presence of side chain charge but must also reflect the unique complementarity at the protein−membrane interface. In summary, the annexin data do not fit a simple electrostatics-based model but are better described by a model in which macroscopic binding comprises both nonspecific and specific interactions.

REFERENCES

1. Moss, S. E., Ed. (1992) *The Annexins*, Portland Press, London.
2. Raynal, P., and Pollard, H. B. (1994) *Biochim. Biophys. Acta 1197*, 63−93.
3. Swairjo, M. A., and Seaton, B. A. (1994) *Annu. Rev. Biophys. Biomol. Struct. 23*, 193−213.
4. Seaton, B. A., Ed. (1996) *Annexins: Molecular Structure to Cellular Function*, R. G. Landes Co., Austin TX.
5. Voges, D., Berendes, R., Burger, A., Demange, P., Baumeister, W., and Huber, R. (1994) *J. Mol. Biol. 238*, 199−213.
6. Olofsson, A., Mallouh, V., and Brisson, A. (1994) *J. Struct. Biol. 113*, 199−205. Ames, B. N., and Dubin, D. T. (1960) *J. Biol. Chem. 235*, 769−775.
7. Concha, N. O., Head, J. F., Kaetzel, M. A., Dedman, J. R., and Seaton, B. A. (1992) *FEBS Lett. 314*, 159−162.
8. Pigault, C., Follenius-Wund, A., Schmutz, M., Freyssinet, J. M., and Brisson, A. (1994) *J. Mol. Biol. 236*, 199−208.
9. Tait, J. F., Gibson, D., and Fujikawa, K. (1989) *J. Biol. Chem 264*, 7944−7949.
10. Blackwood, R. A., and Ernst, J. D. (1990) *Biochem. J. 266*, 195−200.
11. Huber, R., Schneider, M., Mayr, I., Römisch, J., and Pâques, E. P. (1990) *FEBS Lett. 275*, 15−21.
12. Huber, R., Berendes, R., Burger, A., Schneider, M., Karshikov, A., Luecke, H., Römisch, J., and Pâques, E. P. (1992) *J. Mol. Biol. 223*, 683−704.
13. Concha, N. O., Head, J. F., Kaetzel, M. A., Dedman, J. R., and Seaton, B. A. (1993) *Science 261*, 1321−1324.
14. Meers, P., and Mealy, T. (1994) *Biochemistry 33*, 5829−5837.
15. Swairjo, M. A., Concha, N. O., Kaetzel, M. A., Dedman, J. R., and Seaton, B. A. (1995) *Nat. Struct. Biol. 2*, 968−974.
16. Thiel, C., Weber, K., and Gerke, V. (1991) *J. Biol. Chem. 266*, 14732−14739.
17. Thiel, C., Osborn, M., and Gerke, V. (1992) *J. Cell Sci. 103 (Part 3)*, 733−742.
18. Jost, M., Weber, K., and Gerke, V. (1994) *Biochem. J. 298*, 553−559.
19. Travé, G., Cregut, D., Lionne, C., Quignard, J. F., Chiche, L., Sri Widada, J., and Liautard, J. P. (1994) *Protein Eng. 7*, 689−696.
20. Travé, G., Quignard, J. F., Lionne, C., Sri Widada, J., and Liautard, J. P. (1994) *Biochim. Biophys. Acta 1205*, 215−222.
21. Nelson, M. R., and Creutz, C. E. (1995) *Biochemistry 34*, 3121−3132.
22. Mira, J. P., Dubois, T., Oudinet, J. P., Lukowski, S., Russo-Marie, F., and Geny, B. (1997) *J. Biol. Chem. 272*, 10474−10482.
23. Sopkova, J., Renouard, M., and Lewit-Bentley, A. (1993) *J. Mol. Biol. 234*, 816−825.
24. Meers, P., and Mealy, T. (1993) *Biochemistry 32*, 5411−5418.
25. Follenius-Wund, A., Piemont, E., Freyssinet, J. M., Gerard, D., and Pigault, C. (1997) *Biochem. Biophys. Res. Commun. 234*, 111−116.
26. Meers, P., Ernst, J. D., Duzgunes, N., Hong, K. L., Fedor, J., Goldstein, I. M., and Papahadjopoulos, D. (1987) *J. Biol. Chem. 262*, 7850−7858.
27. Bazzi, M. D., and Nelsestuen, G. L. (1991) *Biochemistry 30*, 7961−7969.
28. Hope, M. J., Bally, M. B., Webb, G., and Cullis, P. R. (1985) *Biochim. Biophys. Acta 812*, 55−65.
29. Ames, B. N., and Dubin, D. T. (1960) *J. Biol. Chem. 235*, 769−775.
30. Swairjo, M. A., Roberts, M. F., Campos, M. B., Dedman, J. R., and Seaton, B. A. (1994) *Biochemistry 33*, 10944−10950.
31. Fritsma, G. A. (1989) in *Hemostasis and thrombosis in the clinical laboratory* (Corriveau, D. M., and Fritsma, G. A., Eds.) pp 92−124, J. P. Lippincott Co., Philadelphia.
32. Seaton, B. A., Head, J. F., Kaetzel, M. A., and Dedman, J. R. (1990) *J. Biol. Chem. 265*, 4567−4569.
33. Otwinowski, Z. (1993) DENZO: An oscillation data processing program for protein crystallography, Yale University, New Haven.
34. Brünger, A. (1993) *X-PLOR Version 3.1 Manual*, Yale University, New Haven.
35. Brünger, A. (1992) *Nature 335*, 472−475.
36. Jones, T. A., and Kjeldgaard, M. (1992) *O—The Manual*, Uppsala, Sweden.
37. *CCP4: A suite of programs for protein crystallography* (1979) (SERC collaborative computing project No. 4, Daresbury Laboratory, Warrington U.K.
38. Laskowski, R. A., MacArthur, M. W., Moss, D. S., and Thornton, J. M. (1993) *J. Appl. Crystallogr. 26*, 282−291.
39. Andree, H. A. M., Stuart, M. C., Hermans, W. Th., Reutelingsperger, C. P. M., Frederik, P. M., and Willems, G. M. (1992) *J. Biol. Chem. 267*, 17907−17912.
40. Schiffer, M., Chang, C.-H., and Stevens, F. J. (1992) *Protein Eng. 5*, 213-214.
41. Meers, P. (1990) *Biochemistry 29*, 3325−3330.
42. Snitko, Y., Koduri, R. S., Han, S. K., Othman, R., Baker, S. F., Molini, B. J., Wilton, D. C., Gelb, M. H., and Cho, W. (1997) *Biochemistry 36*, 14325−14333.
43. Murray, D., Ben-Tal, N., Honig, B., and McLaughlin, S. (1997) *Structure 5*, 985−989.
44. Sheng, Y., Sali, A., Herzog, H., Lahnstein, J., and Krilis, S. A. (1996) *J. Immunol. 157*, 3744−3751.
45. Cutsforth, G. A., Whitaker, R. N., Hermans, J., and Lentz, B. R. (1989) *Biochemistry 28*, 7453−7461.
46. Junker, M., and Creutz, C. E. (1994) *Biochemistry 33*, 8930−8940.
47. Morgan, R. O., and Fernández, M. P. (1995) *Mol. Biol. Evol. 12*, 967−979.
48. Kraulis, P. J. (1991) *J. Appl. Crystallogr. 24*, 946−950.

BI973142N